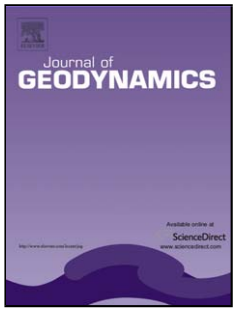

Title: Geokinematics of Central Europe: New insights from the CERGOP-2/Environment Project

Authors: A. Caporali, C. Aichhorn, M. Becker, I. Fejes, L. Gerhatova, D. Ghitau, G. Grenerczy, J. Hefty, S. Krauss, D. Medac, G. Milev, M. Mojzes, M. Mulic, A. Nardo, P. Pesec, T. Rus, J. Simek, J. Sledzinski, M. Solaric, G. Stangl, F. Vespe, G. Virag, F. Vodopivec, F. Zablotskyi

PII: S0264-3707(08)00005-7
DOI: doi:10.1016/j.jog.2008.01.004
Reference: GEOD 832

To appear in: *Journal of Geodynamics*

Received date: 23-1-2007
Revised date: 28-12-2007
Accepted date: 10-1-2008

Please cite this article as: Caporali, A., Aichhorn, C., Becker, M., Fejes, I., Gerhatova, L., Ghitau, D., Grenerczy, G., Hefty, J., Krauss, S., Medac, D., Milev, G., Mojzes, M., Mulic, M., Nardo, A., Pesec, P., Rus, T., Simek, J., Sledzinski, J., Solaric, M., Stangl, G., Vespe, F., Virag, G., Vodopivec, F., Zablotskyi, F., Geokinematics of Central Europe: New insights from the CERGOP-2/Environment Project, *Journal of Geodynamics* (2007), doi:10.1016/j.jog.2008.01.004

Geokinematics of Central Europe: new insights from the CERGOP-2/Environment Project

A.Caporali[1)], C. Aichhorn[2)], M. Becker[3)], I. Fejes[4,5)], L. Gerhatova[6)], D. Ghitau[7)], G. Grenerczy[4,5)], J. Hefty[6)], S. Krauss[2)], D. Medac[8)], G. Milev[9)], M. Mojzes[6)], M. Mulic[10)], A. Nardo[1)], P. Pesec[2)], T. Rus[7)],J. Simek[11)], J. Sledzinski[12)], M. Solaric[8)], G. Stangl[13)] , F. Vespe[14)], G. Virag[4)], F. Vodopivec[15)], F. Zablotskyi[16)]

1) Department of Geosciences, University of Padova, Italy
2) Space Research Institute, Austrian Academy of Sciences, Graz, Austria
3) Institut für Physikalische Geodäsie, Technische Universität Darmstadt, Germany
4) Institute of Geodesy, Cartography and Remote Sensing, Satellite Geodetic Observatory, Penc, Hungary
5) MTA Research Group for Physical Geodesy and Geodynamics, Budapest, Hungary
6) Department of Theoretical Geodesy, Slovak University of Technology, Bratislava, Slovakia
7) Technical University of Civil engineering, Bucharest, Romania
8) Faculty of Geodesy, University of Zagreb, Croatia
9) Central Laboratory of Geodesy, Bulgarian Academy of Sciences, Sofia, Bulgaria
10) Department of Geodesy, Faculty of Civil Engineering, University of Sarajevo, Bosnia Hercegovina
11) Research Institute on Geodesy, Topography and Cartography, Zdby, Czech Republic
12) Institute of Geodesy and Geodetic Astronomy, Warsaw Institute of Technology, Poland
13) Federal Office of Metrology and Surveying, Graz, Austria
14) Centro di Geodesia Spaziale 'G. Colombo, Agenzia Spaziale Italiana, Matera, Italy
15) Faculty of Civil and Geodetic Engineering, University of Ljubljana, Slovenia
16) Chair of Geodesy and Astronomy, Lviv Polytechnic National University, Ukraine

Keywords: GPS Geodesy, Central European Geodynamics, Central European Tectonics, Stress and Strain in Central Europe

Abstract

The Central European Geodynamics Project CERGOP/2, funded by the European Union from 2003 to 2006 under the 5th Framework Programme, benefited from repeated measurements of the coordinates of epoch and permanent GPS stations of the Central European GPS Reference Network (CEGRN), starting in 1994. Here we report on the results of the systematic processing of available data up to 2005. The analysis has yielded velocities for some 60 sites, covering a variety of Central European tectonic provinces, from the Adria indenter to the Tauern window, the Dinarides, the Pannonian Basin, the Vrancea seismic zone and the Carpathian Mountains. The estimated velocities define kinematical patterns which outline, with varying spatial resolution depending on the station density and history, the present day surface kinematics in Central Europe. Horizontal velocities are analyzed after removal from the ITRF2000 estimated velocities of a rigid rotation accounting for the mean motion of Europe: a ~2.3 mm/yr north-south oriented convergence rate between Adria and the Southern Alps that can be considered to be the present day velocity of the Adria indenter relative to the European foreland. An eastward extrusion zone initiates at the Tauern Window. The lateral eastward flow towards the Pannonian Basin exhibits a gentle gradient from 1-1.5 mm/yr immediately east of the Tauern Window to zero in the Pannonian Basin. This kinematic continuity implies that the Pannonian plate fragment recently suggested by seismic data does not require a specific Eulerian pole. On the southeastern boundary of the Adria microplate, we report a velocity drop from 4-4.5 mm/yr motion near Matera to ~1 mm/yr north of the Dinarides, in the southwestern part of the Pannonian Basin. A positive velocity gradient as one moves south from West Ukraine across Rumania and Bulgaria is estimated to be 2 mm/yr on a scale of 600-800 km, as if the crust were dragged by the counterclockwise rotation along the North Anatolian Fault Zone. This regime apparently does not interfere with the Vrancea seismic zone: earthquakes there are sufficiently deep (> 100 km) that the brittle deformation at depth can be considered as decoupled from the creep at the surface. We conclude that models of the Quaternary tectonics of Central and Eastern Europe

should not neglect the long wavelength, nearly aseismic deformation affecting the upper crust in the Romanian and Bulgarian regions.

Introduction

The easternmost seismogenic area of Europe is connected to the Carpathians, the mountain belt which extends east from the Alps into Central Europe. The Carpathians were formed in the Miocene as a result of collision between the Eurasian plate and several microplates. Back arc and intra arc extensional basins, which accompanied the collision, are the Pannonian Basin, separating the Carpathians from the Dinarides, and the Transylvanian Basin. Horváth and Royden (1981) pointed out the occurrence of thinning and updoming of the lithospheric mantle, thermal contraction and related subsidence in a post-rift phase of basin formation. In general, uplift, denudation and sedimentation are competing processes in the Transdanubian zone and all need to be considered to understand the neotectonic pattern of this part of Central European (Fodor et al., 2005). Convergence with the Nubia plate is mirrored by seismic activity at considerable depth (>100 km) in the Vrancea seismic zone, and to some extent by the kinematics of the Adria microplate and the Pannonian Basin. Based on the GPS velocities computed by Grenerczy et al. (2000; 2005) and Grenerczy and Kenyeres (2006), Fodor et al. (2005) identified three kinematic units in Central Eastern Europe: a western unit, located east of the Southern Eastern Alps and responding to the updoming in the Tauern Window by lateral escape; a northeastern unit, interacting directly with the northeastern Carpathians, which accommodate the eastward motions; and a southeastern unit interacting with the Southern Carpathians, which contains the Vrancea seismic zone. All these three units are characterized by an eastward motion accommodated by sinistral faults to the north and dextral faults to the south. Very little is known on the kinematics and the deformation east and southeast of the Carpathians, where the European platform is generally assumed to be substantially stable. This assumption is certainly consistent with the lack of brittle deformation implied by the low to absent surface seismicity in this area. However, coupling with the counter clockwise rotation

of the Anatolian block in the South is not unlikely and it cannot be excluded a priori that the European platform south of the Carpathians is itself undergoing active stretching.

In this paper we intend to make a more detailed analysis of the present day kinematics of the Alpine – Carpathian – Pannonian – Dinaric region. As part of the activities of the Central European GPS Geodynamic Reference Network (CEGRN) (Barlik et al., 1994, Fejes, 2006), GPS campaigns were carried out from 1994 to 2006 involving both permanent and epoch stations across Central Europe. Systematic reprocessing of the campaigns, and additional campaigns done under the EU sponsored Projects CERGOP and CERGOP/2, have enabled us to extend the work of Grenerczy and Kenyeres (2006) and detail the horizontal velocities of sites, their uncertainty, and the velocity field associated with the horizontal motion. The potential of GPS data for a better understanding of the 4-D topographic evolution of the orogens and intraplate regions of Europe has recently been reviewed by Cloetingh et al. (2007) in the frame of the TOPO EUROPE Project. The average velocity field resulting from the interpolation of a dense network of GPS stations can provide a unique link among several processes controlling the evolution of Central Europe. In this sense the CEGRN network, covering several European Nations for more than ten years and with increasing spatial resolution, has a greater potential than previous research based on more localized networks.

2. Tectonic structure

2.1 Kinematics

The tectonic history of the Carpathian-Pannonian system is dominated by plate interactions to its south (Figure 1). The break up of Pangea in the early Mesozoic created the Tethys Ocean and an irregular continental margin across what was then southern Europe. This rifting also produced a collage of microplates between the major paleo-Eurasian and paleo-Afro-Arabian plates. The tectonic development of the region generally reflects the relative movements between the large

plates, and the complications posed by the intervening microplates produced the puzzling geology in the Mediterranean region (Anderson and Jackson, 1987). The tectonic evolution of the Carpathian Mountains - Pannonian Basin system continues to the present. Active seismicity is concentrated at depths of up ~200 km in the Vrancea region north of Bucharest (Stephenson et al., 1996).

During the Cenozoic, the Carpathian Arc evolved to assume its strongly arcuate shape (Csontos, 1995). This block underwent both rotations and translations. The subduction of oceanic areas between this block and paleo-Europe produced considerable Neogene volcanism (Seghedi et al., 2004). The resulting arc-related terranes were accreted to Paleozoic terranes to the north and east, resulting in the formation of the Carpathian fold and thrust belts. Back arc extension played a major role in the formation of the Pannonian Basin. Lithospheric anisotropy inherited from the time of subduction can concentrate strain and induce large-scale deformation far away from the active plate margins (Matenco et al., 2007). During Miocene times, subduction and volcanism were gradually extinguished along the Carpathian arc from west to east and then to the south. The migration of the young Carpathian orogenic belt was limited by the edge of the European Platform. A slab can now only be detected at the southeastern bend of the Carpathian arc, at the Vrancea zone (Oncescu, 1984), where present-day deformation is being investigated by dense local GPS surveys. (Dinter et al., 2001, van der Hoeven et al., 2003).

2.2 Crust

The Adriatic indenter, the Eastern Alps, the European Foreland and the Pannonian Basin differ significantly in their crustal structure. The crustal and lithospheric thickness of the Central European foreland ranges between 40 km to 50 km and 180 km to 200 km respectively (Majdanski et al., 2007). Thickening of the crust is observed in the region of the Tauern Window and Friuli, North East Italy, consistently with the isostatic compensation of the topography.

Beneath that domain the lithosphere forms a root reaching a depth of 220 km (Scarascia & Cassinis, 1997). In contrast, the crust and lithosphere of the Pannonian Basin is thin and warm. Through intense Oligocene - Miocene stretching, the crust was thinned to 22-30 km (Horváth, 1993). High heat flow causes a weak crust and is responsible for a loss of lithospheric strength. The heat flow pattern changed significantly from the Oligocene to the present. In Miocene times extensional tectonics accompanied by the exhumation of large hot core complexes (e.g. Tauern Window; Ratschbacher et al. 1991, Neubauer et al., 2000) and magmatic activity, especially within the Pannonian Basin and along the Periadriatic Lineament, caused elevated surface heat flows. The average present day heat flow of the European Platform is around 60mW m^{-2}. In contrast, an average heat flow of 90 mW m^{-2} makes the Pannonian crust and lithosphere weak in comparison to the cold and thick equivalents of the European Platform (Lenkey, 1999). These thermal properties of the crust affect the strength envelope and are an important factor in the analysis of the deformation implied by the GPS velocities.

2.3 Stress

The counter clockwise rotation of the Adriatic microplate around a pole at 46.1°N 6.9°E with an angular velocity of 0.35 deg/Myr (Caporali and Martin, 2000; Grenerczy et al., 2005) represents a major source for tectonic stress within the Alpine-Pannonian region. The stress regime changed from the Eocene to the present. Several stages of deformation patterns have been worked out for the northern Eastern Alps (Peresson and Decker, 1997), for the southern Alps (Castellarin et al., 2000, Fellin et al., 2002), the Vienna and Danube basins (Fodor, 1995), and the Pannonian Basin and western Carpathians. The paleostress patterns from the domain of the Eastern Alps and the Pannonian Basin are similar, while the southern Alps show significant differences.

The maximum horizontal stress (S_H) orientation of the Central European stress province rotates gradually and remains radial relative to the Carpathian arc (Figure 2) (Reinecker and Lenhardt,

1999).The Bohemian Massif shows a Central European stress pattern. This rigid block is flanked by units in the south and the east with a lower rheological strength. This rheology contrast is reflected by the radial stress pattern around the southern Bohemian Massif (Reinecker and Lenhardt, 1999; Bada et al., 1998). The stress trajectories are perpendicular to boundaries of high rheological contrast. The S_H of the Bohemian basin and the Dinarides is NE oriented and therefore normal to the orogen (Gruenthal and Stromeyer, 1992).The stress pattern can be traced into the Pannonian Basin (Horváth and Cloetingh, 1996). Within the basin the stress trajectories diverge. The western part of the Pannonian Basin belongs to the Central European stress province. The orientation of S_H in the eastern part of the Pannonian Basin is NNE to NE while the central Pannonian Basin shows a S_H orientation of WNW to NW.

The Eastern part of the Pannonian Basin represents a transition zone between the Western European stress province and the Dinarides stress province, the latter displaying predominantly E-W compression. The Adriatic stress province is characterized by north-south compression. As shown in the portion of Figure 2 referring to the middle – lower Adriatic Sea, S_H progressively changes from NNE-SSW to ENE-WSW. These changes reflect the transition to the Pannonian-Dinaric stress province (Reinecker and Lenhardt, 1999; Bada et al., 2007).

3. The CERGOP Velocities and Velocity Field in Central Europe

The locations of epoch and permanent GPS long-term observations of sites in Central Europe, the Eastern Alps, Dinarides and Balkans forming the CEGRN network are shown in Figure 1. The permanent GPS stations in the region were used to ensure that the resulting realization of the Terrestrial Reference System is as rigorously as possible aligned and scaled to the state of the art International Terrestrial Reference Frame ITRF2000 (Stangl, 2002; Becker et al., 2006; Hefty, 2006). Network coordinates and their covariance matrices from all eight CEGRN epoch campaigns solutions are used here as input for estimating the velocity field. The epoch-wise observing

campaigns of CEGRN, comprising five 24-hour simultaneous sessions, have been performed since 1994. Initially, they were realised annually, in 1994, 1995, 1996, 1997, and then bi-annually in the late spring in 1999, 2001, 2003 and 2005.

The processing strategy was identical for all 8 epoch campaigns. Campaigns from 1994 to 2001 were reprocessed in 2002 with improved models (Becker et al., 2002a,b). The main features of the computation strategy were: processing in daily intervals (0-24h UT), celestial reference frame realised by IGS orbits and corresponding Earth Rotation Parameters (ERPs), 10º elevation cut-off, station zenith delays estimated at hourly intervals, Niell (1996) mapping function, and elevation dependent weighting. Models of relative phase centre variations were consistent with IGS values. The number of observed stations included in CEGRN was gradually increased. The first epoch campaign in 1994 included 23 stations. In 1995 the network comprised 32 CEGRN stations (9 of them observed already permanently at that time) and included a further 4 IGS reference stations to enable reliable referencing to ITRF. The CERGOP 2005 campaign included 95 sites.

The characteristics of combined solutions of the eight CEGRN observation campaigns are summarised in Table 1. For velocity estimation we used the ADDNEQ2 program of the Bernese GPS software, version 5.0 (Hugentobler et al., 2004). The solution was validated by an independent velocity estimation model developed at the Slovak University of Technology using the error and weighting scheme described of Hefty et al. (2004). The combination of CEGRN solutions from various epochs is referenced to both ITRF2000 and ITRF2005 by constraining coordinates and velocities of a set of selected IGS sites using their variances and covariances from the ITRF2000 and ITRF2005 solutions respectively (Boucher et al., 2004; Altamimi et al., 2007). The differences between the two reference systems are negligible from the point of view of geokinematics. The ITRF2000 velocities are used here.

The selection of the reference sites was determined by the requirement that their velocities are obtained from a combination of at least two space techniques (GPS and VLBI and/or SLR). This

criterion is met by the IGS stations BOR1, GRAZ, KOSG, MATE, WTZR, ONSA and ZIMM, which were included in CEGRN epoch campaign processing. Velocities at 52 non-reference sites were then determined on the basis of 1014 coordinate observations. The estimated CEGRN velocities and their uncertainties expressed in a geocentric reference system are summarised in Table 2.

The uncertainties depend mainly on the time span of observations (sites with the longest observation history cover 11 years), then on the number of incorporated campaigns (from 3 to 8) and on the quality and repeatability of site epoch observations.

To obtain information about the intraplate velocity field, model velocities for Eurasia were removed from the estimated velocities. We used the APKIM 2000 (Drewes, 1998) plate motion model, which is based on VLBI, SLR and GPS observations. The resulting intraplate velocities (with the APKIM model velocities removed) and their RMS errors are summarized in Table 3 and in Figure 3.

4. Velocity field in a regular grid

As is evident from Figure 3 the distribution of sites with known velocities is not uniform; also remarkable are the differences in uncertainties of velocities at individual sites. To obtain information suitable for geo-kinematical modelling we interpolated the discrete velocities to a regular grid. Grid spacing must be defined consistently with the data distribution and the uncertainties.

For horizontal velocity interpolation we used a Least Squares Collocation. The covariance of the velocities can be approximated by a function $C(d)$

$$C(d) = \sigma_{0s}^2 \exp\left(-c^2 d^2\right) \qquad (1)$$

where d is spherical distance between the measured and interpolated points expressed in degrees, $\sigma_{0s}{}^2$ is the variance of the velocities and c is the reciprocal of the scale distance for decorrelation of velocity pairs. The exponential covariance is normally used because it is finite and has zero derivative at the origin, is isotropic and has a minimum of adjustable parameters.

A best fit to the variogram of the velocities yields $\sigma_{0s} = 2$ mm/yr and c = 0.35 deg^{-1}. The graphical representation of the used covariance function is in Figure 4. The characteristic distance of decorrelation of approximately 300 km agrees with earlier independent estimates in the Alpine Mediterranean area, and with the flexural wavelength of a 30 km thick crust (Caporali et al., 2003, Caporali, 2006).

Application of the least squares collocation method to the interpolation of horizontal velocities v_{pred} is based on the simple relation

$$\mathbf{v}_{pred} = \mathbf{C}_S \mathbf{C}_v^{-1} \mathbf{v}_{obs} \qquad (2)$$

where C_S is covariance matrix of signal, and v_{obs} is the vector of CEGRN velocities reduced for APKIM and for a mean value, and C_v is their covariance matrix. The mean velocity is restored after interpolation. The geographical distribution of sites with CEGRN velocities as well as their uncertainties is inhomogeneous, so the optimum choice of grid for interpolated velocities is not trivial. We choose a (East x North) 2º x 1º grid, as a compromise between data density and spatial resolutions over most of the study area.

Figure 5 shows the interpolation on the 2º x 1º grid. The interpolation procedure takes rigorously into account the uncertainties and stochastic relationships among the observed velocities, so that error ellipses of the interpolated velocities, not shown in the figure, can also be estimated.

5. Discussion

5.1 Adria, Dinarides and Pannonian Basin

The Adria microplate is the most active, fastest moving, major source of tectonic stress that dominantly shapes the deformation of South Central Europe. The independence of Adria from Nubia and Eurasia was tested and proved; F-ratio tests (Stein and Gordon, 1984) were performed for several subsets of sites believed to be on Adria. The two plate model assumption Adria-Eurasia turned out to be valid for all of the tests; their motion and boundaries were also outlined and suggested further fragmentation (Ward, 1994; Calais et al., 2002; Grenerczy et al., 2005). The strain distribution along the Italian part was further analyzed by Caporali et al., (2003) and the extensional strain across the Appenines was determined (Hefty, 2005). Figure 3 shows that the CEGRN stations MATE, DUBR, HVAR and SRJV in the Adriatic region have well constrained velocities and the general convergence towards the Dinarides is clearly depicted in Figure 6. A much more detailed picture will benefit from the upcoming 20 Bosnian GPS sites (Mulic et al., 2006) and a few additional sites in Serbia.

The stations in the northern part of the Adriatic Sea (MEDI, UPAD, BASO, LJUB, MALI) define a dominant velocity in a northerly direction with an average magnitude of 2 mm/yr. The Austrian stations GRMS, SBGZ and GRAZ show eastward velocities, consistent with earlier results (Grenerczy et al., 2000; 2005; D'Agostino et al., 2005; Vrabec et al., 2006, Caporali et al., 2006). Accordingly, stations within, or near, the Pannonian Basin have velocities about 2 mm/year generally oriented to the east (HUTB, DISZ, PENC, STHO, KAME).

The Adria microplate appears as a wedge intruding into the southern part of the Eastern Alps, and causing a lateral, eastwards extrusion towards the Pannonian Basin acting as an unconstrained stress sink. Recent results in seismic profiling have evidenced a vertical step of the Moho at the transition between the Alpine and Pannonian domains, suggesting the existence of a Pannonian plate fragment (Brückl et al., 2007). The lateral flow describing the extrusion is clearly visible in Figure 6 and it appears rather continuous. Hence, if the hypothesis of a Pannonian plate fragment is justified from

the crustal viewpoint, this cannot yet be confirmed from the kinematical viewpoint with the available data. The Alpine and Pannonian domains seem to share the same velocity pattern and an Eulerian pole specific for the Pannonian plate fragment seems at present unnecessary.

Moving further north of parallel 48N, the velocities become small and randomly oriented, suggesting that a kinematically 'stable' European platform starts roughly north of the Carpathians.

5.2 The Carpathian Arc

The CEGRN network has several sites in this region operating since 1995. Balkan stations situated in Bulgaria (SOFI, HARM) and Romania (MACI, BUCU, BUCA) have velocities oriented to the south and southeast. SOFI and BUCU/BUCA belong to the EUREF network and are well constrained. The magnitude of velocities ranges from 2 to 4 mm/year and all the vectors exceed the 2σ intervals. Other Romanian stations (MACI, IAS3, TIS3) have a shorter tracking history. Because of their uncertainty comparable or larger than the estimated velocity, they are treated as random noise by the collocation filter. Figure 5 shows a number of interesting features of the velocity field in the Eastern Carpathians, Transylvania and the Wallachian region that includes the border between Bulgaria and Rumania. In Transylvania the velocities appear significantly different from zero, suggesting that this area, located just west of the Vrancea seismic zone, could be subject to active deformation. South and east of the Carpathian Arc, velocities increase by approximately 2 mm/yr across a 600 km profile as one moves south (Figure 6), indicating a long wavelength extensional regime. Previous measurements (Kotzev, 2001, 2006), based on four years of data (1996-2000), gave preliminary indications that an extensional regime characterizes the Wallachian area, southwards to the Hellenic arc. Our data confirm that the area south of the Carpathians is undergoing active stretching because of a positive gradient north to south. This stretching seems to decrease moving west, where the velocity field gradually decreases (Burchfiel et al., 2006) and then reverses its direction in the area of Macedonia and Albania, suggesting an area of right lateral shear.

The combination of the CEGRN data with the Italian and Greek data could shed more light on this area of active deformation.

6. Conclusions

The data we have presented cover a sizable part of Central and Eastern Europe where deformation and seismicity are moderate. Consequently, to discriminate a geokinematic signal out of noise requires a network such as CEGRN. We are able to confirm previous knowledge, and add some new results. With reference to Figure 6, the interaction of Adria with the Southern Alps and the Dinarides involves contraction in different directions, N–S in the first case and SW-NE in the second case. The velocity drops by a factor of two, the northesast drift towards the Dinarides involving a larger slip rate, as high as 3.5 – 4 mm/yr. The eastwards tectonic motion towards the Pannonian Basin is continuous and involves small velocity drops, of the order of 1 - 1.5 mm/yr. This continuity at the surface is not mirrored at the depth of the Moho, where a jump suggests a Pannonian plate fragment separated from the Alpine domain. Overall velocities are small and random north of the 48 N, which can be considered stable in the sense that there is no consistent, collective kinematics. A N–S velocity pattern suggests a stretching crust in the area of Romania and Bulgaria. This stretching is not incompatible with reverse faulting seismicity in the Vrancea seismic zone. Earthquakes there take place at intermediate depths, and decoupling between crustal stretching at the surface and convergence below is implied. The cause for this long wavelength stretching of the crust, which is aseismic in the sense that it is not accommodated by one or more active faults, is to be found in a coupling with the counter rotation of the Anatolian block, resulting in a dragging effect. Hence, the convergence with the Nubia plate in the Hellenic arc has a long wavelength tail which extends just south of the Carpathian arc. Geophysical indicators of stress (Figure 2) are patchy in this area, but where they exist they appear compatible with an extensional regime. Hence, models of Quaternary tectonics of Central and Eastern Europe should consider the portion of Europe north of the Carpathians as moving rigidly. The Alpine Carpathian Pannonian

region is undergoing active deformation, as well as the Romanian – Bulgarian upper crust with its long wavelength, nearly aseismic deformation profile likely to be controlled by the motion of Anatolia and convergence with the Nubian Plate in the Hellenic arc.

Acknowledgements

Particular thanks are due to Dr. Peter Pesec, who coordinated the CERGOP-2/Enviromental project among 14 participating institutions and provided scientific and financial reports in due times for Brussels. This work was supported by the EU EVK2-CT-2002-00140 grant. The Hungarian team acknowledges the support of OTKA T042900 and F68497 and MŰI TP 108 grants. Two anonymous referees provided constructive criticisms which helped to improve the original manuscript. The assistance from the Editorial Office is gratefully acknowledged.

References

Altamimi, Z., Collilieux, X., Legrand, J., Garayt, B., Boucher, C., 2007. ITRF2005: A new release of the International Terrestrial Reference Frame based on time series of station positions and Earth Orientation Parameters, J. Geophs. Res., 112, B09401, doi:10.1029/2007JB004949.

Anderson, H., Jackson, J., 1987. Active tectonics of the Adriatic region, Geophys. J. R. astr. Soc., 91, 937-983.

Bada, G., Cloetingh, S. A. P. L., Gerner, P., Horváth, F., 1998. Sources of recent tectonic stress in the Pannonian region: inferences from finite element modelling, Geophys. J. Int., 134, 87–102.

Bada, G., Horváth, F., Dövényi, P., Szafián, P., Windhoffer, G., Cloetingh, S., 2007**,** Present-day stress field and tectonic inversion in the Pannonian basin, Global and Planetary Change 58,165-180 ,TOPO-EUROPE: the Geoscience of Coupled Deep Earth-Surface Processes, doi:10.1016/j.gloplacha.2007.01.007

Barlik M., Borza T., Busics I., Fejes I., Pachelski W., Rogowski J., Sledzinski J., Zielinski J., 1994. Central Europe Regional Geodynamics Project. Reports on Geodesy No.2(10), 7-24.

Becker, M., Cristea, E., Figurski, M., Gerhatova, L., Grenerczy, G., Hefty, J., Kenyeres, A., Liwosz, T., Stangl, G., 2002a. Central European intraplate velocities from CEGRN campaigns, Reports on Geodesy., l(61), 83-91.

Becker M., Caporali A., Figursky, M., Grenerczy, Gy., Kenyeres, A., Hefty, J., Marjanovic, M., Stangl, G., 2002b. A Regional ITRF Densification by Blending Permanent and Campaign Data - The CEGRN campaigns and the Central European Velocity Field. Vistas for Geodesy in the New Millennium, eds. J. Ádám, K.-P. Schwarz, International Association of Geodesy Symposia, Vol. 125, pp. 53-58, Springer-Verlag, Berlin-Heidelberg-New York.

Becker, M., Drescher, R., Schönemann, E., Gutwald, J., 2006. Improvements in CEGRN station monitoring and in the CEGRN velocity field. Proceedings of final CERGOP-2 Working Meeting, Graz, Austria, July 13. - 14., Reports on Geodesy No. 3 (78) , in press.

Boucher, C., Altamimi, Z., Sillard, P., Feissel-Vernier, M., 2004. The ITRF 2000. IERS Technical note No. 31. Frankfurt am Main, Verlag des Bundesamtes für Kartographie und Geodäsie.

Brückl, E., Bleibinhaus, F., Gosar, A., Grad, M., Guterch, A., Hrubcovà, P., Randy Keller, G., Majdanski, M., Sumanovac, M., Tiira, T., Yliniemi, J., Hegedus, E., Thybo, H., 2007. Crustal structure due to collisional and escape tectonics in the Eastern Alps region based on profiles Alp01 and Alp02 from the ALP 2002 seismic experiment, J. Geophys. Res., 112, B06308, doi:10.1029/2006JB004687

Burchfiel, B.C., King, R.W., Todosov, A., Kotzev, V., Durmurdzanovd, N., Serafimovskid, T., Nurcee, B., 2006. GPS results for Macedonia and its importance for the tectonics of the Southern Balkan extensional regime, Tectonophysics, 413, 239-248, doi:10.1016/j.tecto.2005.10.046

Calais, E., Nocquet, J.M., Jouanne, F., Tardy, M., 2002. Current strain regime in the Western Alps from continuous GPS measurements, 1996-2001, Geology, 30-7, 651-654.

Caporali, A., Martin, S., 2000. First results from GPS measurements on present day alpine kinematics. J. of Geodyn., 30, 275-283.

Caporali A., Martin S, Massironi M., 2003. Average strain rate in the Italian crust inferred froma a permanent GPS network - II.Strain rate vs. Seismicity and Structural Geology. Geophysical Journal International, 155, 254-268 ISSN: 0956-540X.

Caporali A., Massironi, M., Nardo, A., 2006. Constraining the seismic budget of Adria indentation and the dynamics of fault interaction with geodetic strain rate data, paper presented at Wegener 2006 meeting, Sept., 2006, Nice, France.

Caporali, A., 2006. Adding geodetic strain rate data to a seismogenic context, Boll. Geofis. Teor. Appl. 47(3), 455-479.

Castellarin, A., Cantelli, L., Fesce, A.M., Mercier, J.L., Picotti, V., Pini, G.A., Prosser, G., Selli, L., 2000. Alpine compressional tectonics in the Southern Alps. Relationships with the N-Apennines. Annales Tectonicæ, VI (1), 62-94.

Cloetingh, S.A.P.L., Ziegler, P.A., Bogaard, P.J.F., Andriessen, P.A.M., Artemieva, I.M., Bada, G., van Balen, R.T., Beekman, F., Ben-Avraham, Z., Brun, J.-P., Bunge, H.P., Burov, E.B., Carbonell, R., Facenna, C., Friedrich, A., Gallart, J., Green, A.G., Heidbach, O., Jones, A.G., Matenco, L., Mosar, J., Oncken, O., Pascal, C., Peters, G., Sliaupa, S., Soesoo, A., Spakman, W., Stephenson, R.A., Thybo, H., Torsvik, T., de Vicente, G., Wenzel, F., Wortel M.J.R., and TOPO-EUROPE Working Group, 2007. TOPO-EUROPE: The geoscience of coupled deep Earth-surface processes, Global and Planetary Change 58, 1-118, doi:10.1016/j.gloplacha.2007.02.008

Csontos, L., 1995. Tertiary tectonic evolution of the Intra-Carpathian area: a review, Acta Vulcanologica, 7(2) 1–13.

D'Agostino, N., Cheloni, D., Mantenuto, S., Selvaggi, G., Michelini, A., Zuliani D., 2005. Strain accumulation in the Southern Alps (NE Italy) and deformation oat the northeastern boundary of Adria observed by CGPS measurements. Geophys. Res. Letters 32, L19306, doi:10.1029/2005GL024266.

Dinter, G., Nutto, M., Schmitt, G., Schmidt, U., Ghitau, D., Marcu, C., 2001. Three dimensional deformation analysis with respect to plate kinematics in Romania, Reports on Geodesy, 2(57): 29-42.

Drewes, H., 1998. Combination of VLBI, SLR and GPS determined station velocities for actual plate kinematics and crustal deformation models. In: Forsberg, R., Feissel, M., Dietrich, R. (eds.): Geodesy on the Move, Gravity, Geoid, Geodynamics, and Antarctica, IAG Symposia Vol. 119, Springer, pp. 377-382.

Fellin, S., Martin, S., Massironi, M., 2002. Polyphase tertiary fault kinematics and Quaternary reactivation in the Central-Eastern Alps (Western Trentino). Journal of Geodynamics 34, 31-46.

Fejes I., 2006. Consortium for Central European GPS Geodynamic Reference Network (CEGRN Consortium). In The Adria Microplate: GPS Geodesy, Tectonics, and Hazards, eds. N. Pinter, G. Grenerczy, J. Weber, S. Stein, D. Medak, Springer, Dordrecht, 183-194.

Fodor, L., 1995. From transpression to transtension: Oligocene-Miocene structural evolution of the Vienna basin and the East Alpine – Western Carpathian junction, Tectonophysics, 242, 151–182.

Fodor, L., Bada, G., Csillag, G., Horva´th, E., Ruszkiczay-Ru¨ digger, Z., Palota´s, K., Sý´khegyi, F., Tima´r, G., Cloetingh, S., Horva´th, F., 2005. An outline of neotectonic structures and morphotectonics of the western and central Pannonian basin, Tectonophysics 410, 15– 41.

Grenerczy, Gy., Kenyeres, A., Fejes, I., 2000. Present crustal movement and strain distribution in Central Europe inferred from GPS measurements, J. of Geophys. Res. 105B9, 21,835-21,846.

Grenerczy, Gy., Sella, G., Stein, S., Kenyeres , A., 2005. Tectonic implications of the GPS velocity field in the northern Adriatic region, Geophys. Res. Lett., 32, L16311, doi:10.1029/2005GL022947.

Grenerczy, Gy., Kenyeres, A., 2006. GPS velocity field from Adria to the European Platform, in The Adria Microplate: GPS Geodesy, Tectonics, and Hazards, Editors: N. Pinter, G. Grenerczy, D. Medak, S. Stein, and J. C. Weber, Springer, Dordrecht, pp. 321-334.

Gruenthal, G., Stromeyer, D., 1992. The recent crustal stress field in Central Europe: Trajectories and finite element modeling. J. of Geophys. Res. 97B8, 11,805–11,820.

Hefty J., Gerhátová L., Igondová M., Kováè M., Hrèka M., 2004. The Network of Permanent GPS Stations in Central Europe as the Reference for CERGOP Related Activities, Reports on Geodesy No. 2. (69) 115-123.

Hefty J., 2005. Kinematics of Central European GPS Geodynamic Reference Network as the Result of Epoch Campaigns During Nine Years, Reports on Geodesy No. 2. (73), 23-32 .

Hefty, J., 2006. Work-package 7 of the CERGOP-2/Environment: GPS data analysis and the definition of reference frame. Final report: April 2003 – July 2006. Reports on Geodesy (in print) .

Horváth, F., Royden, L., 1981. Mechanism for the formation of the intra Carpathian basins: a review, Earth Evolution Sciences 3, 307-316.

Horváth, F., 1993. Towards a mechanical model for the formation of the Pannonian basin., Tectonophysics, *226*, 333-357.

Horváth, F., Cloetingh, S. A. P. L., 1996. Stress-induced late-stage subsidence anomalies in the Pannonian basin, Tectonophysics, 266, 287–300.

Hugentobler, U., Dach, R. and Fridez, P. (eds) 2004. Bernese GPS software, Version 5.0. Draft. Bern: Astronomical Institute, University of Berne.

Kotzev, V., Nakov, R., Burchfiel, B.C., King, R., Reilinger, R., 2001. GPS study of active tectonics in Bulgaria: results from 1996 to 1998, Journal of Geodynamics, 31, 189-200, doi:10.1016/S0264-3707(00)00027-2

Kotzev, V., Nakovb, R., Georgiev, Tz., Burchfiel, B.C., King, R.W., 2006. Crustal motion and strain accumulation in western Bulgaria ,Tectonophysics, 413, 127-145, doi:10.1016/j.tecto.2005.10.040

Lenkey, L., 1999. Geothermics of the Pannonian basin and its bearing on the tectonics of basin evolution, PhD dissertation, Vrije Universiteit, Amsterdam, The Netherlands, p. 1-215.

Majdański, M., Kozlovskaya, E. , Grad, M. and SUDETES 2003 Working Group, 2007. 3D structure of the Earth's crust beneath the northern part of the Bohemian Massif, Tectonophysics 437, Issues 1-4, 17-36, doi:10.1016/j.tecto.2007.02.015

Matenco, L., Bertotti, G., Leever, K., Cloetingh, S., Schmid, S.M., Tărăpoancă, M., Dinu,C., 2007. Large-scale deformation in a locked collisional boundary: Interplay between subsidence and uplift, intraplate stress, and inherited lithospheric structure in the late stage of the SE Carpathians evolution, Tectonics, 26, TC4011, doi:10.1029/2006TC001951.

Mulic M., Bilajbegovic, A., Altiner, Y., 2006. Study of the effects of processing strategy variations on GPS position estimates, Geophysical Research Abstracts, Vol. 8, 04734, European Geosciences Union.

Neubauer, F., Fritz, H., Genser, J., Kurz, W., Nemes, F., Wallbrecher, E., Wang, X., Willingshofer, E., 2000. Structural evolution within an extruding wedge: model and application to the Alpine-Pannonian system, in: Urai, J., Lehner, F., and van Zee, W. (Eds.): Aspects of tectonic faulting (Festschrift in Honour of Georg Mandl), Springer, 141–153.

Niell, A.E., 1996. Global mapping functions for the atmosphere delay at radio wavelengths, J. of Geophys. Res. 101B2, 3227-3246.

Oncescu, M.C., 1984. Deep structure of the Vrancea region, Romania, inferred from simultaneous inversion for hypocenters and 3-D velocity structure, Annales Geophysicae, 2, 23-28.

Peresson, H., Decker, K., 1997. The Tertiary dynamics of the northern Eastern Alps (Austria); changing palaeostresses in a collisional plate boundary, Tectonophysics, 272, 125–157.

Ratschbacher, L., Frisch, W., Linzer, H.-G., Merle, O., 1991. Lateral extrusion in the Eastern Alps, part 2. Structural analysis, Tectonics, 10, 257–271.

Reinecker, J., Lenhard, W. A., 1999. Present-day stress field and deformation in eastern Austria, Int. Jour. Earth Sci., 88, 532– 550.

Reinecker, J., Heidbach, O., Tingay, M., Sperner, B., Müller, B., 2005. The release 2005 of the World Stress Map (available online at www.world-stress-map.org).

Scarascia, R., Cassinis, R., 1997. Crustal structures in the central- eastern Alpine sector: a revision of the available DSS data. Tectonophysics, 271, 157-188.

Seghedi, I., Downes, H, Szaka´cs, A., Mason, P. R.D., Thirlwall, M. F., Ros_u, E., Pe´cskay, Z., Ma´rton, E., Panaiotu, C., 2004. Neogene–Quaternary magmatism and geodynamics in the Carpathian–Pannonian region: a synthesis, Lithos 72 , 117–146.

Stangl, G., 2002. Creating a common CEGRN solution. The rules behind. Reports on Geodesy, 1 (61), 23-25.

Stein, S., and Gordon, R., 1984. Statistical tests of additional plate boundaries from plate motion inversions, EPSL, 69, 401-412.

Stephenson, R.A., Wilson, M., de Boorder, H., Starostenko, V., 1996. EUROPROBE Intraplate Tectonics and Basin Dynamics of the Eastern European Platform - Preface, Tectonophysics, 268, i-iv.

Vrabec, M., Preseren, P.P., Stopar, B.,2006. GPS study (1996–2002) of active deformation along the Periadriatic fault system in northeastern Slovenia: tectonic model, Geologica Carpathica 57, 57-65.

van der Hoeven, A.G.A., Ambrosius, B.A.C., Spakman, W., Mocanu, V., 2003. Crustal motions in the Eastern Carpathians (Vrancea) measured by GPS, Geophysical Research Abstracts, 5: 03918.

Ward, S., 1994. Constraints on the seismotectonics of the central Mediterranean from Very Long Baseline Interferometry, Geophys. J. Int., 11, 441-452.

Figure captions

Figure 1. Major morphological units of Continental Europe, the Mediterranean and the Hellenic arc. TW = Tawern Window; EA= Eastern Alps, BM = Bohemian Massif, PB = Pannonian Basin, Di = Dinarids, Ap = Apennines, AdS = Adriatic Sea, Ca = Carpathians, VSZ = Vrancea Seismic Zone, Wa = Wallachia, TS = Transylvania. Superimposed are the stations of the CEGRN network. Red circles indicate permanent stations which are part also of the European Permanent Network EPN; red inverted triangles indicate permanent CEGRN Stations; red stars indicate campaign (epoch) CEGRN stations. In the insert: EF = European Foreland, AI = Adria Indenter, PL = Periadriatic

Lineament, SV = Schio Vicenza line. The black arrow indicates the direction of indentation of the Adriatic wedge. The indentation is accommodated by the sinistral strike slip on the West, called the Schio Vicenza line, which however shows no historical seismicity.

Figure 2. Stress in Europe from a combination of geophysical data under the International Lithospheric Project (Reinecker et al., 2005). Data referring to depth <50km and quality better than D are plotted. Regimes: TF = thrust fault; NF= normal fault; SS= strike slip. Digital Earth Model: GTOPO30 of the National Oceanic and Atmospheric Administration. Decimation: 1/5.

Figure 3. Intraplate horizontal velocities with 2σ error ellipses, obtained from CEGRN velocities by removing the corresponding APKIM 2000 velocities.

Figure 4. Covariance function of signal used for interpolation of CEGRN velocity field.

Figure 5. Interpolation of CEGRN horizontal velocities into (E x N) 2º x 1º grid, by least squares collocation. Error ellipses are 1σ. PF indicates the Pannonian fragment, defined by a Moho uplift of some 10 km (Brueckl et al., 2007).

Figure 6. Kinematical interpretation representing the closure of the southern Adria towards the Dinarids, the northwards indentation of the Adria plate fragment, the eastward escape of the Tauern window towards the Pannonian basin, and the southward stretching of the Bulgarian-Rumanian crust. The drag of the Anatolian plate, which counterrotates relative to the Eurasian plate, is a likely explanation. Focal mechanisms are in red for depths up to 35 km, in black for deeper earthquakes.

Table captions

Table 1. Main features of CEGRN campaigns analysed in this paper

Table 2. Velocities of CEGRN sites observed three or more epochs expressed in geocentric coordinate system, number of campaigns, time span covered by epoch campaigns. Reference frame is ITRF2000. Velocities and their uncertainties are in mm/year.

Table 3. Velocities of CEGRN sites observed more than 3 epochs evaluated in the reference frame ITRF2000 reduced with the APKIM model and expressed in the local coordinate system East, North . Units are mm/yr.

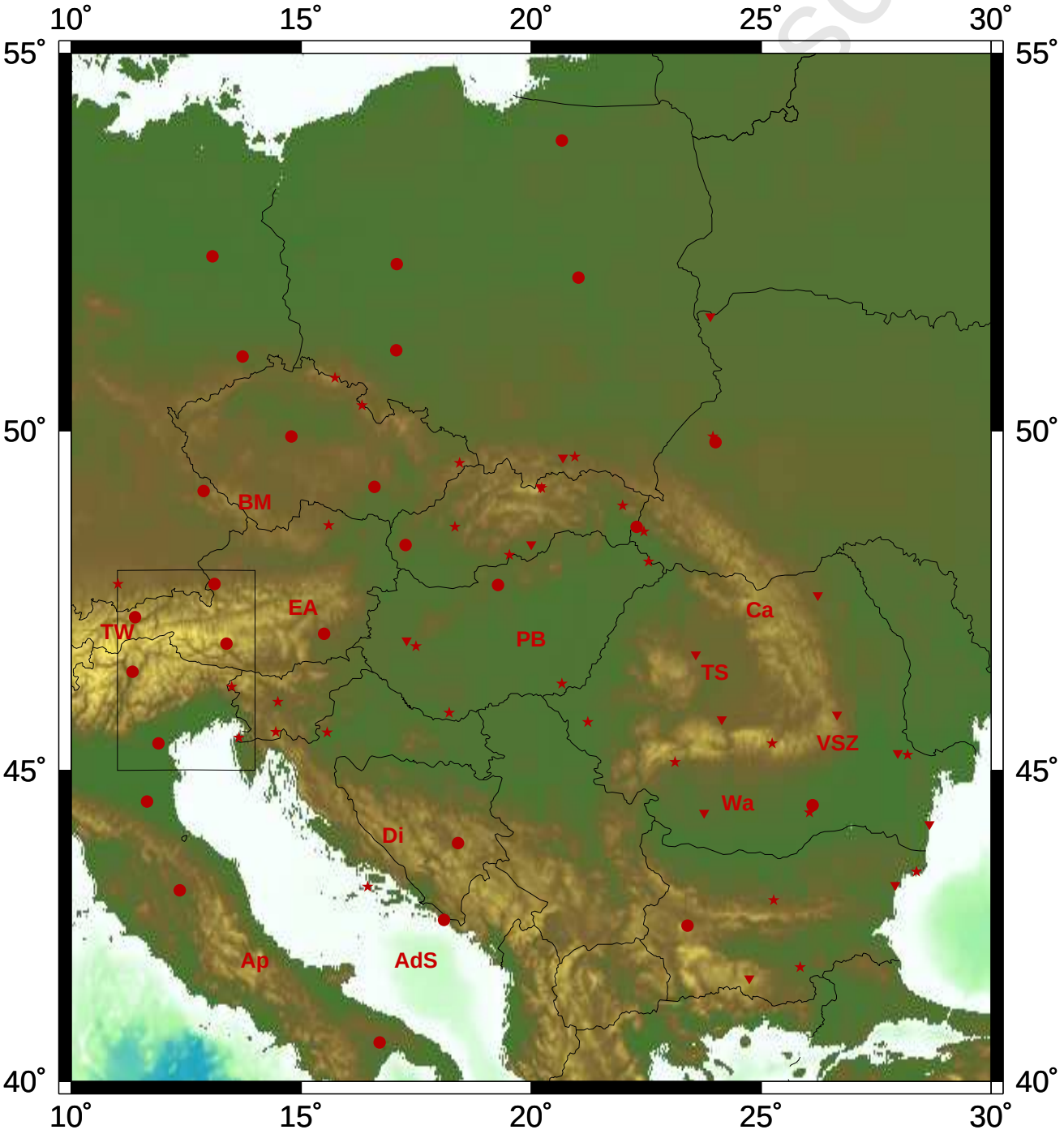
10°
15°
20°
25°
30°
55°
50°
45°
40°
BM
EA
TW
PB
Ca
TS
VSZ
Wa
Di
Ap
AdS

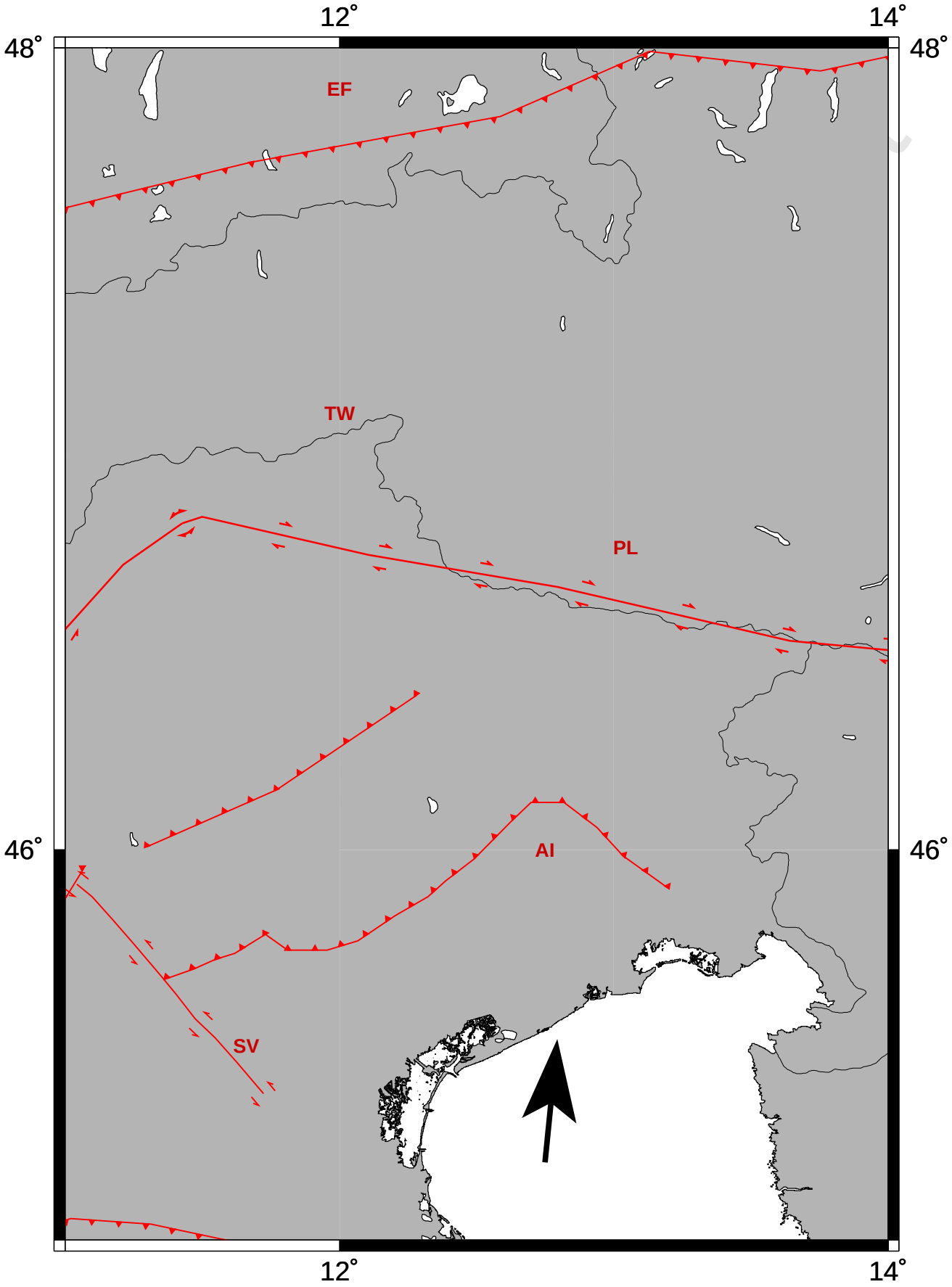

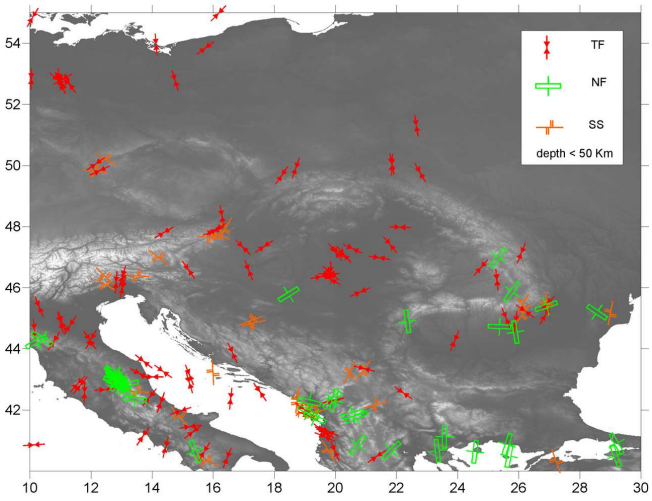

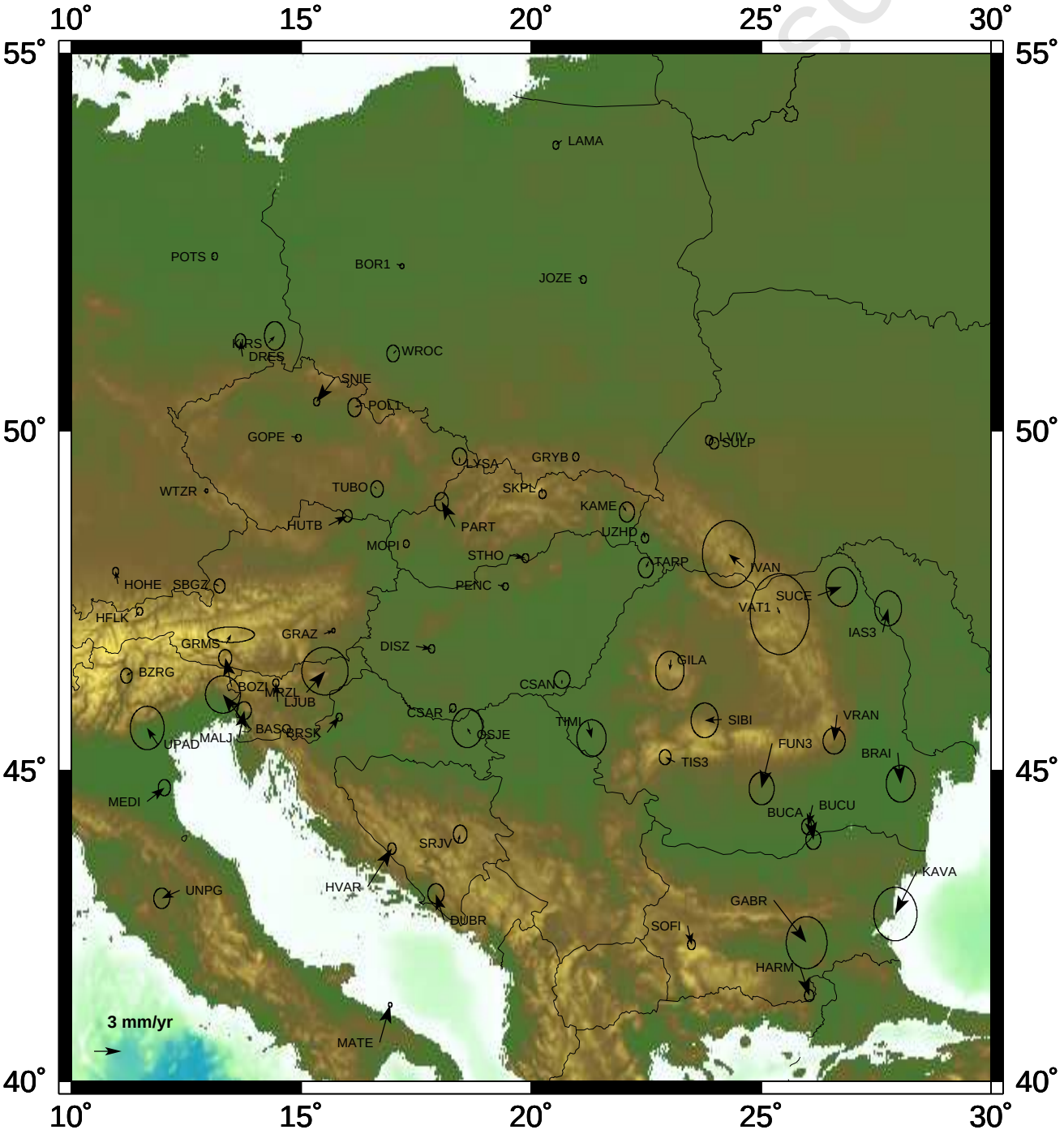
10°
15°
20°
25°
30°
55°
50°
45°
40°
LAMA
POTS
BOR1
JOZE
KRS
DRES
WROC
SNIE
POLI
GOPE
LVIV
SULP
LYSA
GRYB
WTZR
TUBO
SKPL
KAME
HUTB
PART
UZHD
MOPI
STHO
TARP
IVAN
HOHE
SBGZ
PENC
SUCE
VAT1
HFLK
IAS3
GRAZ
GRMS
DISZ
GILA
BZRG
CSAN
BOZ
MRZL
LJUB
CSAR
SIBI
VRAN
TIMI
OSJE
BASO
BRSK
MALJ
UPAD
FUN3
BRAI
TIS3
MEDI
BUCA
BUCU
SRJV
KAVA
UNPG
HVAR
GABR
DUBR
SOFI
HARM
3 mm/yr
MATE

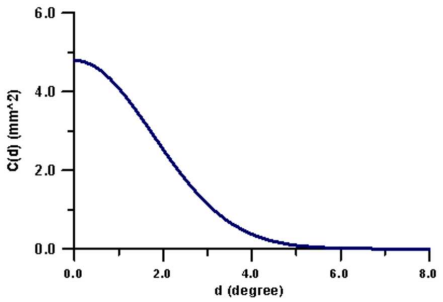

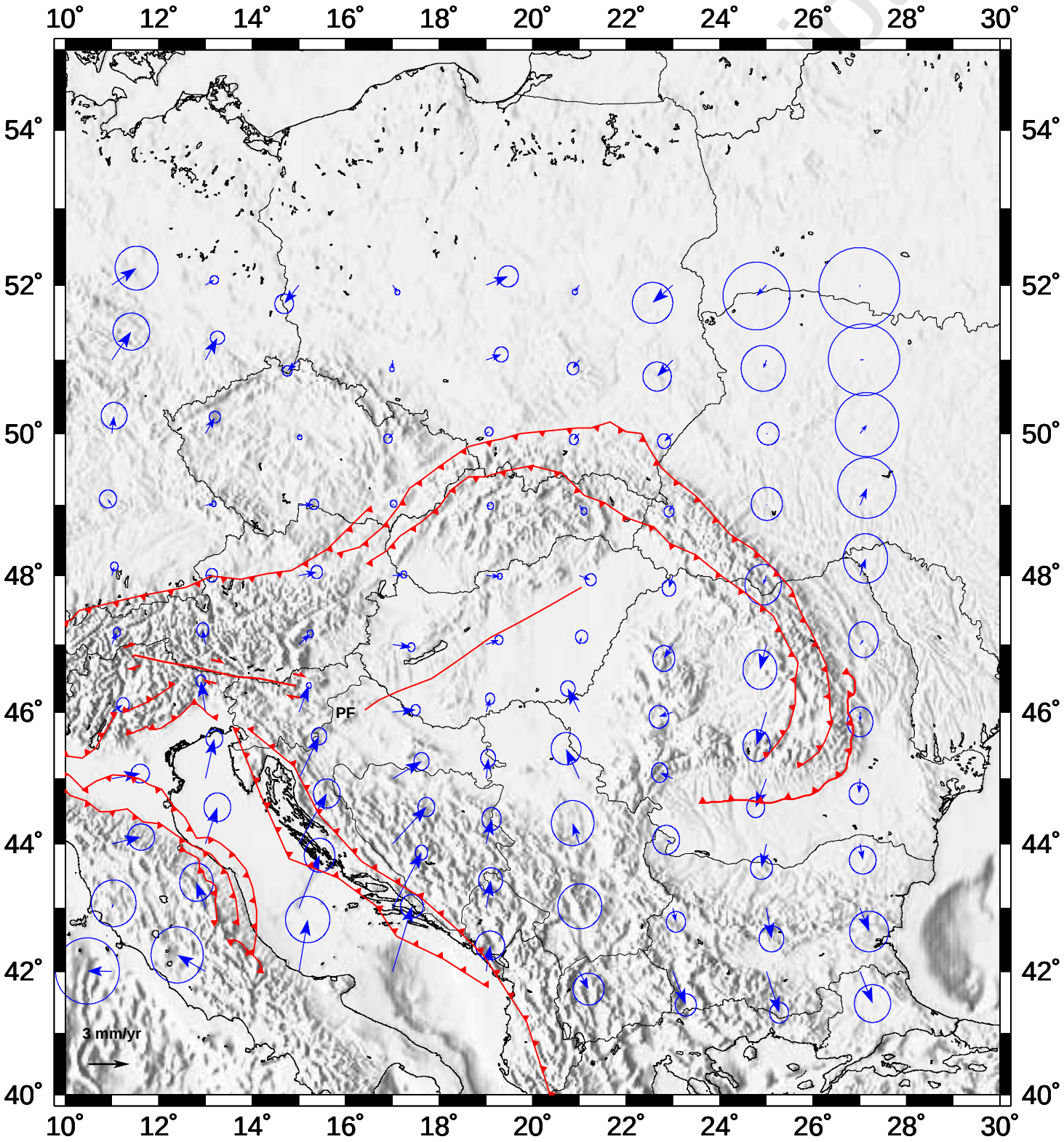

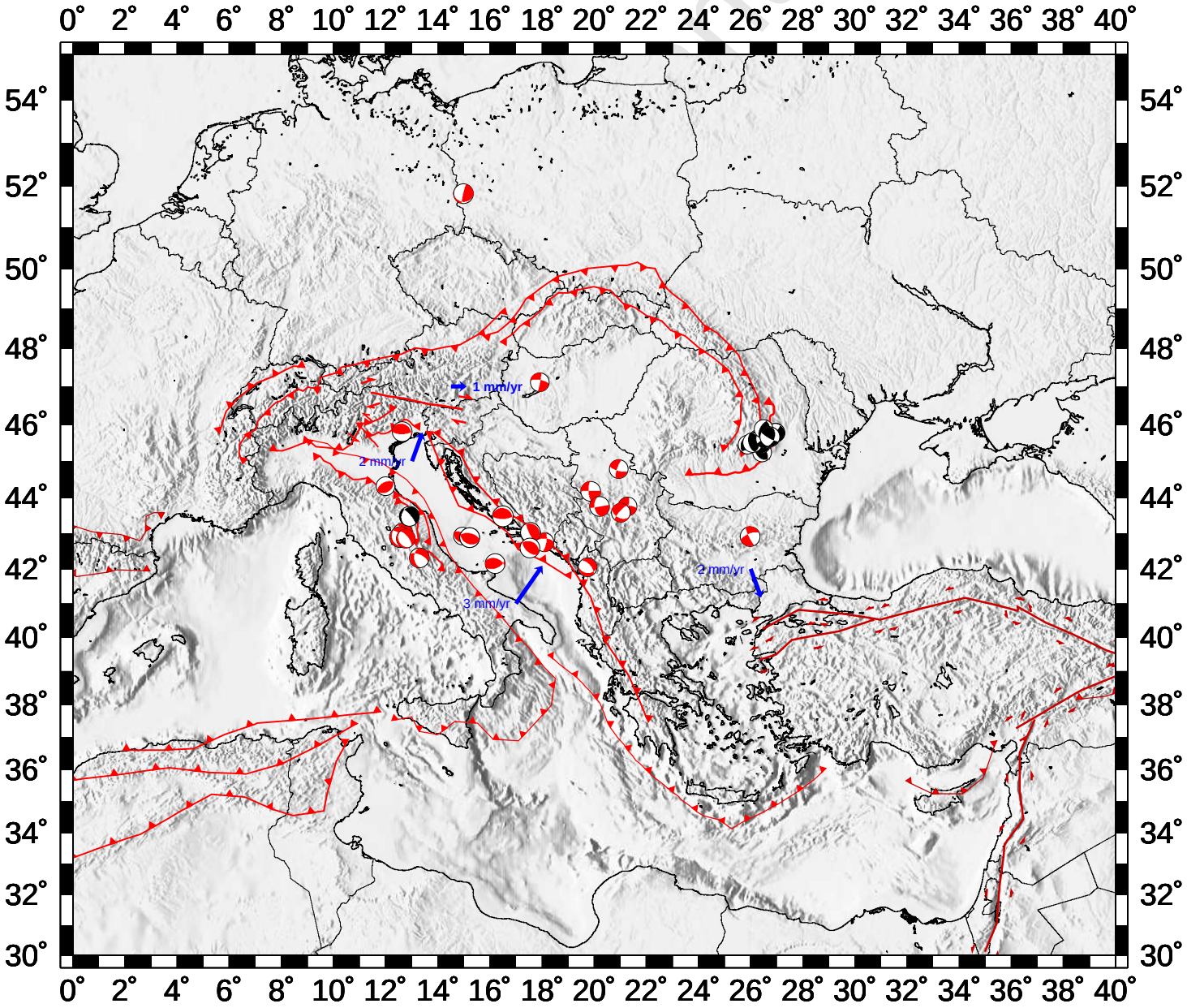

Observing campaign	Epoch of observation	No. of processed sites in the final solution	No. of solutions forming the network combination	RMS of unit weight for the combined solution (m)
CEGRN'94	1994.34	27	3	0.0023
CEGRN'95	1995.41	36	3	0.0029
CEGRN'96	1996.45	37	3	0.0030
CEGRN'97	1997.43	45	4	0.0026
CEGRN'99	1999.46	61	3	0.0024
CEGRN'01	2001.47	55	2	0.0027
CEGRN'03	2003.46	72	4	0.0024
CEGRN'05	2005.47	95	5	0.0016

Site	No of campaigns	Time span (years)	v_X	σ_{VX}	v_Y	σ_{VY}	v_Z	σ_{VZ}
BASO	4	3	-18.0	4.6	14.3	1.5	11.2	4.7
BOR1	8	11	-17.2	0.4	16.1	0.2	7.2	0.6
BOZI	4	6	-18.8	3.3	16.1	1.0	10.3	3.5
BRSK	8	11	-18.9	1.1	19.4	0.4	8.9	1.2
BUCA	6	10	-13.5	2.3	20.0	1.1	10.2	2.5
BUCU	4	6	-18.2	2.9	16.6	1.5	5.4	3.1
BZRG	4	6	-15.7	3.5	16.9	1.0	7.9	3.7
CSAN	4	6	-18.0	3.5	17.2	1.6	8.1	3.8
CSAR	8	11	-18.2	1.2	17.1	0.5	8.5	1.3
DISZ	8	11	-18.4	1.1	19.5	0.4	6.5	1.3
DRES	4	6	-12.0	2.3	17.3	0.8	15.5	2.8
DUBR	3	4	-22.1	5.8	14.7	2.3	7.3	5.6
FUN3	4	6	-6.8	3.6	21.4	1.8	14.1	4.0
GILA	4	4	-31.2	4.5	11.0	2.0	-8.5	5.1
GOPE	8	11	-16.2	0.9	17.5	0.3	8.5	1.1
GRAZ	8	11	-17.6	0.3	18.0	0.1	8.1	0.4
GRMS	4	4	-15.7	8.1	21.8	2.4	11.6	8.9
GRYB	8	11	-18.4	1.1	16.0	0.4	7.2	1.3
HARM	4	9	-18.2	1.9	18.0	0.9	5.3	2.0
HFLK	6	10	-14.0	1.7	18.1	0.5	10.5	1.8
HOHE	7	11	-13.9	1.1	16.7	0.3	12.9	1.2
HUTB	8	11	-17.9	2.0	18.2	0.7	8.4	2.4
HVAR	5	8	-24.6	1.8	18.8	0.6	7.1	1.7
IAS3	3	4	-28.8	4.0	11.7	2.1	0.5	4.8
JOZE	8	11	-17.8	1.0	16.2	0.4	7.7	1.4
KAME	4	6	-18.6	3.1	16.4	1.3	6.8	3.7
KIRS	5	5	-17.3	3.0	16.6	1.0	8.0	3.8
KOSG	8	11	-13.5	0.3	16.6	0.1	9.7	0.5
LAMA	8	11	-18.8	1.0	13.8	0.4	4.7	1.4
LJUB	8	11	-16.5	1.1	16.6	0.4	11.0	1.2
LVIV	7	10	-17.0	1.4	15.9	0.6	8.8	1.8
LYSA	4	6	-16.2	2.7	17.1	1.2	9.8	3.2
MACI	3	3	-24.7	4.1	14.6	2.2	3.9	4.7
MALJ	4	6	-19.9	3.5	16.6	1.1	8.5	3.6
MATE	7	11	-18.9	0.3	19.0	0.1	13.0	0.4
MEDI	4	6	-18.6	3.7	18.1	1.1	9.3	3.7
METS	8	11	-16.0	0.3	14.8	0.2	8.6	0.6
MOPI	8	11	-14.9	1.0	17.3	0.4	10.7	1.2
ONSA	8	11	-13.6	0.2	14.8	0.1	9.4	0.4
PART	4	6	-19.2	2.7	15.1	1.1	10.0	3.1
PENC	8	11	-18.7	0.9	17.1	0.3	6.7	1.0
POL1	4	6	-14.2	2.8	14.9	1.0	11.9	3.4
POTS	7	10	-16.2	1.0	16.2	0.3	7.7	1.3
SBGZ	4	6	-14.1	2.4	18.3	0.8	11.9	2.6
SKPL	8	11	-16.4	1.2	16.8	0.5	8.1	1.5
SNIE	8	11	-14.0	1.0	14.9	0.4	5.9	1.3
SOFI	6	9	-18.4	1.6	18.1	0.7	5.8	1.7
STHO	8	11	-18.3	1.3	17.4	0.5	7.7	1.5
SRJV	4	6	-18.0	4.0	17.4	1.5	9.5	4.0
SULP	5	8	-17.6	1.7	16.0	0.8	8.6	2.2
TARP	4	6	-18.6	3.3	15.5	1.5	6.7	3.8
TIS3	5	9	-12.2	1.8	18.4	0.8	15.3	1.9
TUBO	5	10	-15.8	2.6	17.4	1.0	10.3	3.0
UNPG	3	4	-16.2	2.2	15.8	0.9	8.8	2.8
UPAD	5	6	-17.3	5.4	16.4	1.5	9.1	5.4
UZHD	8	11	-18.2	1.1	16.3	0.5	7.1	1.4
VAT1	3	3	-17.3	12.9	17.1	6.3	8.9	15.3
VRAN	5	8	-31.0	6.4	10.1	3.5	-10.3	7.3
WROC	4	6	-16.2	2.2	15.8	0.9	8.8	2.8
WTZR	6	9	-15.8	0.2	17.1	0.1	8.6	0.4
ZIMM	8	11	-14.0	0.4	18.6	0.2	9.9	0.5

Site	v_n	σ_n	v_e	σ_e
BASO	3.6	1.1	-2.8	1.0
BOR1	-0.3	0.2	0.6	0.2
BOZI	3.3	0.9	-0.7	0.7
BRSK	1.4	0.3	2.4	0.2
BUCA	-3.2	0.6	0.6	0.5
BUCU	-2.6	0.8	-0.4	0.6
BZRG	-0.3	0.9	-0.6	0.7
CSAN	-0.1	1.0	0.5	0.9
CSAR	0.7	0.4	0.3	0.3
DISZ	-0.9	0.4	2.8	0.3
DRES	1.3	0.8	0.1	0.6
DUBR	2.7	1.7	-1.5	1.3
FUN3	-5.2	1.0	-0.7	0.8
GILA	-1.3	1.2	0.0	0.9
GOPE	-0.1	0.3	0.9	0.2
GRAZ	0.4	0.2	1.1	0.1
GRMS	1.0	1.9	4.3	1.4
GRYB	-0.1	0.3	0.2	0.3
HARM	-3.2	0.5	0.4	0.4
HFLK	0.0	0.5	0.4	0.4
HOHE	1.9	0.3	-0.9	0.2
HUTB	0.7	0.6	1.7	0.5
HVAR	3.7	0.5	3.0	0.4
IAS3	2.5	1.0	0.7	0.8
JOZE	-0.2	0.3	0.8	0.3
KAME	-0.5	0.9	0.5	0.7
KIRS	0.7	0.8	0.7	0.6
KOSG	0.3	0.2	0.2	0.1
LAMA	-0.4	0.3	-0.6	0.3
LJUB	1.9	0.3	-0.8	0.3
LVIV	-0.5	0.4	-0.3	0.3
LYSA	0.1	0.9	0.5	0.8
MACI	0.8	1.1	1.0	0.8
MALJ	2.7	0.9	-0.2	0.7
MATE	4.1	0.2	1.1	0.1
MEDI	2.3	1.0	0.6	0.7
METS	-1.4	0.2	1.0	0.2
MOPI	0.0	0.3	0.0	0.2
ONSA	-0.8	0.1	-0.1	0.1
PART	2.9	0.9	-0.7	0.6
PENC	-0.3	0.3	0.9	0.2
POL1	0.9	0.9	-2	0.7
POTS	0.0	0.3	0.4	0.3
SBGZ	0.7	0.8	0.7	0.6
SKPL	-1.0	0.4	0.1	0.3
SNIE	-3.1	0.4	-1.9	0.3
SOFI	-2.3	0.5	0.7	0.4
SRJV	1.0	1.0	0.1	0.8
STHO	0.0	0.4	1.1	0.3
SULP	-0.2	0.5	0.0	0.4
TARP	-0.4	0.9	-0.5	0.7
TIS3	0.4	0.5	-1.0	0.4
TUBO	0.5	0.9	0.6	0.6

UNPG	-2.1	1.7	-2.0	1.4
UPAD	1.6	1.3	-1.1	1.0
UZHD	-0.6	0.4	0.2	0.3
VAT1	-0.8	2.4	0.3	1.7
VRAN	-3.2	2.1	-0.2	1.6
WROC	0.1	0.8	-0.4	0.6
WTZR	0.0	0.1	0.3	0.1
ZIMM	0.4	0.2	0.7	0.2